Mater.Phys.Mech.1 (2000) 54-59

TEM AND STM INVESTIGATIONS ON THE DISCLINATION NATURE OF FRAGMENT BOUNDARY TRIPLE JUNCTIONS

M. Seefeldt

Freiberg University of Mining and Technology, Institute of Physical Metallurgy, Gustav-Zeuner-Straße 5, D-09596 Freiberg, Germany
Present address: Catholic University of Leuven, Department of Metallurgy and Materials Engineering, Willem de Croylaan 2, B-3001 Heverlee, Belgium

Received: October 30, 1999

Abstract. After a short review of recent TEM measurements to characterize partial disclinations in fragment boundary triple junctions in cold-rolled copper, STM results from the same specimens are presented which support a disclination interpretation of the observed fragment structure. The role of the fragment boundary mosaic or of the corresponding immobile partial disclination network in work-hardening is discussed. Although the orientational mismatches around the fragment boundary triple junctions are only small, the disclination contribution dominates work-hardening behaviour at large strains.

1. INTRODUCTION

The substructure development of crystalline metals under cold deformation up to large strains is characterized by the formation of a fragment structure on the mesoscopic scale [1]. Typically, with increasing strain the mean fragment size decreases monotonously starting from the micrometer range, whereas the mean misorientation across the fragment boundaries increases monotonously reaching several degrees [1-3][1]. In contrast to the cell structure, the fragment structure does not saturate[2] and its formation and evolution are quite universal phenomena which are observed in fcc, hdp, and bcc single- as well as polycrystals [1].

While the coexistence of the cell and fragment structures and the evolutions of their characteristic parameters are well investigated [1-3], the defect composition of the fragment boundary mosaic and its influence on work-hardening are not yet completely understood. Especially, to the authors' knowledge, there is no work-hardening model up to now which takes the fragment structure explicitly into account.

Following the Russian school of plasticity, the authors propose the triple junctions of the fragment boundaries to have a disclination character [4-6] and, thus, to be sources of long-range stresses hindering dislocation motion and, thereby, contributing to work-hardening at large strains.

2. NONCOMPENSATED NODES OF FRAGMENT BOUNDARIES

According to experimental observations, a model describing the fragment structure development as well as its coupling to the macroscopic mechanical behaviour requires tools which take into account such collective behaviour of dislocations that results into the formation, spread-out and enlargement of misorientations and into the presence of long-range stresses in the fragment interiors. A model on the substructure development and work-hardening under cold deformation up to large strains suggested by the present authors [7,8] uses disclinations [9,10] as such a tool. Especially, the formation of partial disclination dipoles (PDD) is modelled through incidental non-balanced trapping of neighbouring mobile dislocations of the same Burgers vector into cell walls and by incidental trapping of mobile dislocations with "matching" Burgers vector into preexisting fragment boundaries [8]. The first PDD configuration corresponds to a both-side terminated excess dislocation wall, the second one to a tilt or twist boundary segment with enlarged misorientation. To describe the non-conservative propa-

[1] Hansen and coworkers use the term «cell block» instead of fragment.

[2] Saturation means in this context that average cell structure parameters like cell size, cell wall width, or misorientation do not change any more.

Corresponding author: M. Seefeldt, e-mail: Marc.Seefeldt@mtm.kuleuven.ac.be

© 2000 Advanced Study Center Co. Ltd.

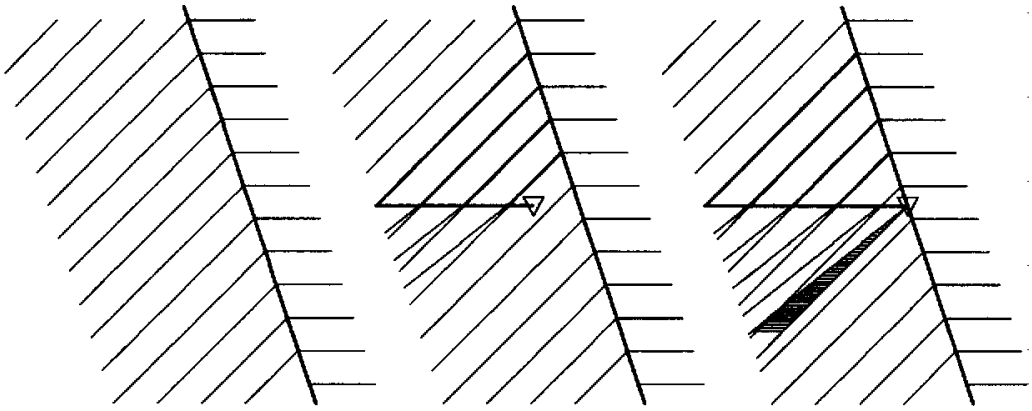

Fig. 1. A propagating partial disclination approaches a preexisting fragment boundary, is locked in this boundary and leaves an orientational mismatch behind.

gation of the partial disclinations of such dipoles along cell walls or fragment boundaries, respectively, the capturing mechanism proposed by Vladimirov and Romanov [10,11] is used.

If a partial disclination propagates like that and approaches a preexisting fragment boundary, then it will rotate the crystal regions to the left and to the right of the growing backward fragment boundary against each other (Fig. 1b). When it is finally locked in the preexisting fragment boundary, an orientational mismatch is left behind (Fig. 1c). This mismatch can be accomodated in two different ways: either "plastically" by generation of an additional dislocation boundary or "elastically" by rotational distortion. In the latter case, the triple junction is a non-compensated node containing a line defect of the disclination type.

3. TEM RESULTS

Since partial disclinations locked in the triple junctions of the fragment boundaries should – at least at low homologous temperatures – be stable under load relaxation, they are suitable objects for an experimental confirmation of the disclination approach used in the above mentioned model. TEM microdiffraction measurements around fragment boundary triple junctions in copper single and polycrystals rolled down to 70% and 50% thickness reduction at room temperature, respectively, showed [12]

– that the product of the three misorientation matrices does not give the identity and
– that the local orientation varies continuously when passing with the electron beam by the node.

Whereas the first observation proves an orientational mismatch, the second one points towards its accomodation by elastic distortion rather than by an additional dislocation boundary. Both items together indicate that the triple junction includes an additional line defect which has – probably beside other contributions [13,14] – a disclination nature. The measured orientational mismatches correspond to Frank vectors of

$$\vec{\omega} = [-0.0292, 0.0094, 0.0052] \text{ with } |\vec{\omega}| = 1.78°, \quad (1)$$

for a node in the single crystal specimen and

$$\vec{\omega} = [-0.0046, -0.0316, 0.0004] \text{ with } |\vec{\omega}| = 1.93°, \quad (2)$$

for a node in the polycrystal specimen. These PD powers are in good agreement with the theoretical expectation of $|\vec{\omega}| \approx 1–3°$ given by Romanov and Vladimirov in [10]. At present, PDD groups in a copper single crystal rolled down to 60% thickness reduction as shown in the TEM micrographs in Figs. 2 and 3 are analysed.

First results indicate that the PDD groups are not fully compensating dipole (Fig. 2) and quadrupole (Fig. 3) configurations, respectively [15].

4. STM RESULTS

Since it is very difficult to find sufficiently large perfect crystal volumes to obtain Kikuchi patterns in the surroundings of the nodes in heavily deformed metals, an additional local characterization method which does not make use of diffraction is desirable. Scanning tunnel microscopy (STM) is such a method. In their pioneering works, Vettegren' et al. [16-20] have studied the profiles of polished surfaces of loaded copper, gold, and molybdenum specimens and found clusters of etch pits. The pits have been explained by the exit of dislocation groups after bursting through barriers on intersecting glide planes, whereas the clusters have been interpreted as an early stage of crack formation [21].

Unfortunately, the STM contrast theory is not yet very well developed. It is known [22] that the strong electric field between the tip and the surface has an etching effect. It is generally admitted that this "field etching" should also result into preferred evaporation

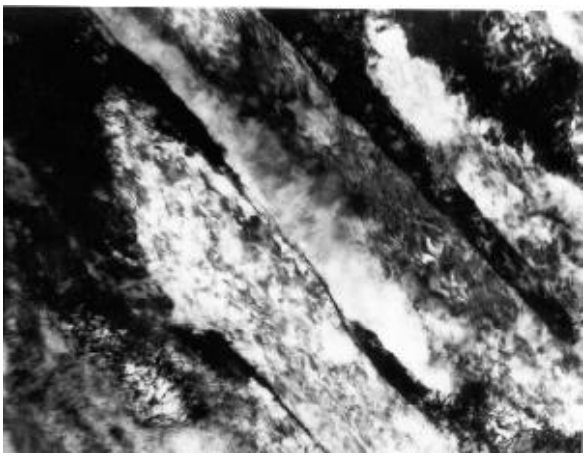

Fig. 2. TEM micrograph of a partial disclination dipole configuration. Copper single crystal rolled down to 60% thickness reduction at room temperature. 2.61×1.90 μm².

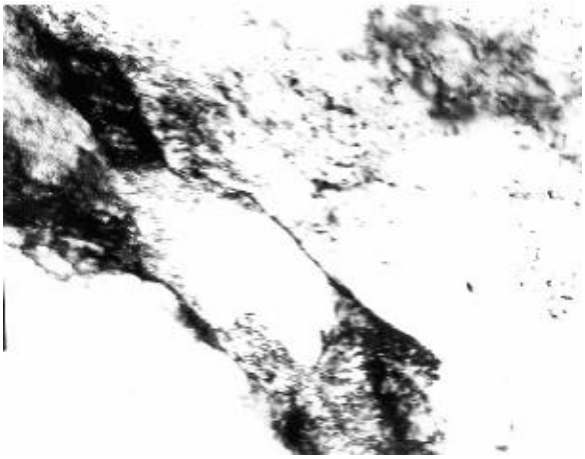

Fig. 3. TEM micrograph of a partial disclination quadrupole configuration. Copper single crystal rolled down to 60% thickness reduction at room temperature. 1.59×1.16 μm².

and/or surface diffusion at high-energy surface regions. From an analogy to Mullins' thermal etching theory [23], one can conclude that etch grooves should arise and deepen at the lines where planar defects like grain boundaries or fragment boundaries reach the surface. Depth and shape *z(x,t)* of the grooves scale with the plane energy γ of the planar defect, e.g. for thermal etching with dominating evaporation and condensation through [23]

$$z(x,t) = -2\tan\beta\sqrt{At}\ \mathrm{ierfc}\left(\frac{x}{2\sqrt{At}}\right) \qquad (3)$$

with β defined by the mechanical equilibrium between the planar defect (e.g. grain boundary) tension and the surface tensions, $2\gamma_{sf}\sin\beta = \gamma_{gb}$, and *A* given by

$$A = \frac{\rho_0\,\gamma_{sf}\,\Omega^2}{(2\pi M)^{1/2}(k_B T)^{2/3}} \qquad (4)$$

with vapour pressure ρ_0 for plain surface, atomic volume Ω, atomic mass *M* and temperature *T*. Fragment boundaries can be approximated as low-angle grain boundaries, so that their plane energy can be expressed through the misorientation, e.g. for a tilt boundary [24]

$$\gamma_\beta = \frac{Gb}{4\pi(1-\nu)}\varphi\left(\ln\frac{b}{r_0} - \ln\varphi\right) \qquad (5)$$

with misorientation φ and dislocation core radius r_0. Thus, at least in the thermal etching analogy, the groove depth and shape are directly related to the fragment boundary misorientation. Correspondingly, "field etching" should also result into notching of etch pits at the points where line defects like dislocations or disclinations reach the surface. Depth and shape of the pits should then scale with the line energy, that means with the powers or with the moduli of the Burgers or Frank vectors, respectively. Although Romanov has given the elastic fields around PDDs reaching the surface [25], there is no etch pit theory up to now, not even for the thermal analogy. Therefore, the following discussion has to remain a qualitative one: If the triple junctions of fragment boundaries include additional high-energy line defects, then the corresponding etch pits should be much deeper than the etch grooves corresponding to the joining fragment boundaries.

For the present work, cut surfaces of copper polycrystals rolled at room temperature have been abraded, polished and treated with the basic alumina OPS be-

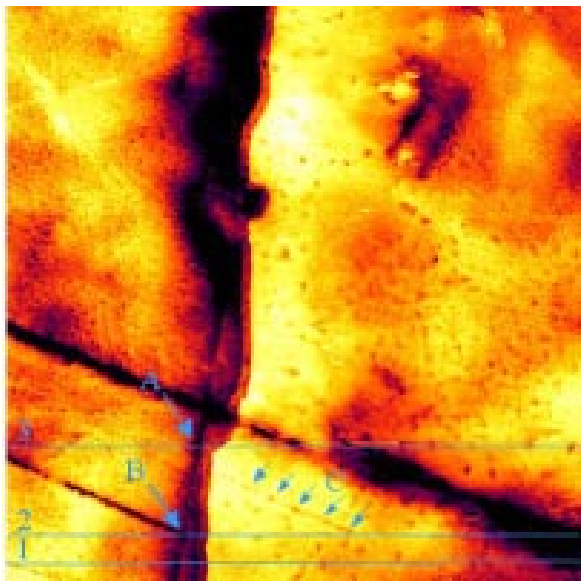

Fig. 4. STM surface profile with fragment boundary grooves. Copper polycrystal rolled down to 70% thickness reduction at room temperature. Arrow "A" marks a splitting point of a fragment boundary, arrow "B" a triple junction, arrows "C" a chain of nearly equidistant shallow etch pits. 5×5 μm². Grey scale from white to black corresponding to 15 nm depth.

fore being investigated with a Nanoscope II STM. Fig. 4 shows a 5×5 μm² surface profile from a copper polycrystal rolled down to 71% thickness reduction. The parallelity of the two grooves on the left (to each other and also to the very much different structure of a chain of nearly equidistant small pits marked with the arrows "C"!), the similarity of the defect structure with the one observed in TEM (confer e.g. [2,26]), especially the band width in the micrometer range and the splitting up of one groove into two neighbouring ones at the point "A" (confer splitting up of dense dislocation walls (DDW) into first generation microbands (MB1), e.g. [2,26]) point to a deformation-induced rather than to a polishing effect.

Fig. 5 gives the scanning profiles for the three lines marked in Fig. 4, line 1 cutting through the two neighbouring ordinary grooves, line 2, in addition to this, cutting through the triple junction marked with "B", and line 3 cutting through the splitting point marked with "A". Obviously, the pits at the triple junctions are deeper than the ordinary grooves by about a factor 2 which might indicate the presence of an additional high-energy line defect, e.g. a partial disclination.

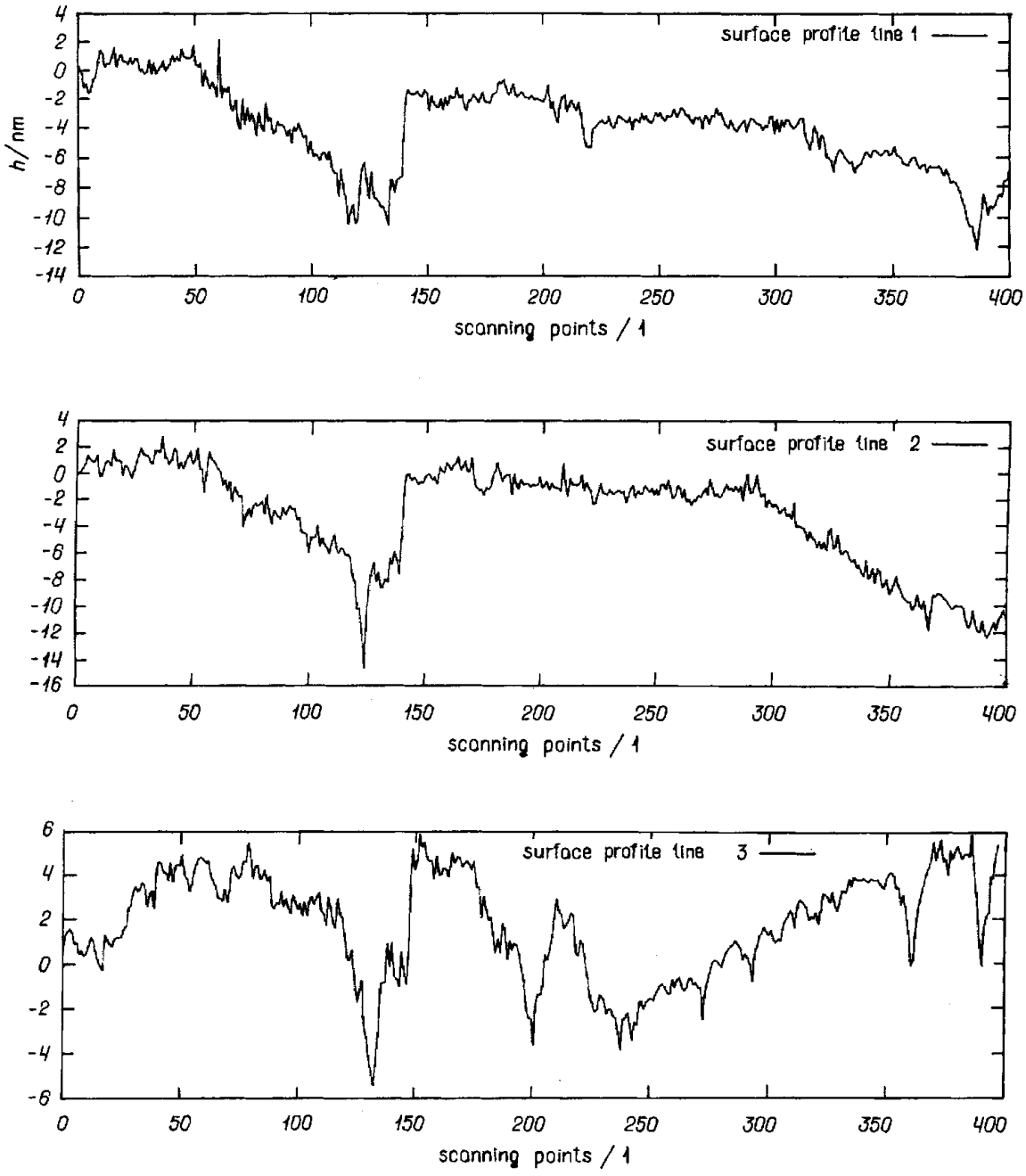

Fig. 5. STM surface profiles along the lines 1-3 in Fig. 4. 400 scaning points correspond to 5 μm.

5. EFFECT ON WORK-HARDENING

In a disclination-based model for the fragment structure development like the one proposed in [7,8], propagating PDDs are immobilized as discussed in section 2 and Fig. 1 – resulting in a mosaic of fragment boundaries or, correspondingly, in a network of immobile partial disclinations in the node lines of this mosaic. The evolutions of the cell wall dislocation density and of the propagating and immobile disclination densities can be described with the equations [8]

$$\frac{dp_c}{d\varepsilon} = I\sqrt{\rho_c} - R\rho_c, \tag{6}$$

$$\frac{d\theta_\rho}{d\varepsilon} = \frac{K_c}{N}\sqrt{\rho_c} + \frac{K_f}{N}\sqrt{\theta_i} - J\sqrt{\theta_i}\theta_\rho, \tag{7}$$

$$\frac{d\theta_i}{d\varepsilon} = J\sqrt{\theta_i}\theta_\rho, \tag{8}$$

including immobilization (*I*-term) of mobile and dynamic recovery (*R*-term) of mobile with cell wall dislocations, PDD generation by incidental non-balanced trapping of *N* neighbouring mobile dislocations into cell walls (K_c-term) and by incidental trapping of mobile dislocations with the "right" Burgers vector into fragment boundaries (K_f-term), and immobilization of propagating PDDs in the network of immobile ones (*J*-term). The coefficients can be estimated from physical models for the elementary processes [7,8]. Whereas the cell wall dislocation density saturates according to the Kocks-type equation (6), the immobile disclination density increases monotonously according to equation (8) – corresponding to a monotonously decreasing mean fragment size.

The cell wall dislocation density is coupled to a flow stress contribution according to

$$\Delta\sigma_\rho = \frac{\xi\alpha Gb}{m_s}\sqrt{\frac{\rho_c}{\xi}}, \tag{9}$$

where m_S is the Schmid factor and ξ denotes the volume fraction of the cell walls. The effect of the immobile disclination density on the flow stress is described by Romanov's and Vladimirov's law [10]

$$\Delta\sigma_\theta = \beta G|\vec{\omega}|. \tag{10}$$

The mean disclination power $|\vec{\omega}|$ is equivalent to the average orientational mismatch around the node lines and may – following the discussion in section 2 and Fig. 1 – be approximated by the mean misorientation φ. Assuming a Poisson-Voronoi geometry of the fragment boundary mosaic, the mean misorientation is calculated by distributing the available excess dislocation density which develops according to (*E*-term describes capturing of mobile dislocations by propagating partial disclinations)

$$\frac{d\rho_{exc}}{d\varepsilon} = K_c\sqrt{\rho_c} + K_f\sqrt{\theta_i} + E\theta_\rho \tag{11}$$

on the total fragment boundary plane area, finally giving [7]

$$\varphi \approx b\rho_{exc} / 1.21\sqrt{\theta_i}. \tag{12}$$

Integration of the evolution equations (6–8) and the flow stress contributions (9–10) shows that the disclination contribution to flow stress dominates the dislocation one starting from a von Mises strain of about 0.9 (parameters for copper at room temperature). Stage III of single crystal plastic deformation can be attributed to cell structure or dislocation work-hardening, stage IV to fragment or disclination work-hardening [7,8].

6. CONCLUSIONS

TEM microdiffraction measurements indicate the presence of line defects of disclination nature in the triple junctions of fragment boundaries. STM shows deep etch pits at the points where the triple junction lines reach the surface — pointing to high-energy line defects in the triple junctions. Although the orientational mismatches remain small, the disclination long-range stress fields do have a significant influence on work-hardening and even dominate the dislocation contribution at large strains.

REFERENCES

[1] V.V. Rybin, *Large Plastic Deformation and the Fracture of Metals* (Metallurgiya, Moskva, 1986) (in Russian).

[2] B. Bay, N. Hansen, D.A. Hughes and D. Kuhlmann-Wilsdorf // *Acta Metall. Mater.* **40** (1992) 205.

[3] Q. Liu, D. Juul Jensen and N. Hansen // *Acta Mater.* **46** (1998) 5819.

[4] V.A. Likhachev and V.V. Rybin // *Izv. Akad. Nauk. SSSR Fiz.* **37** (1973) 2433.

[5] V.I. Vladimirov and I.M. Zhukovskiy // *Fiz. Tverd. Tela* **16** (1974) 346.

[6] V.A. Likhachev and V.V. Rybin // *Fiz. Tverd. Tela* **18** (1976) 163.

[7] M. Seefeldt and P. Klimanek // *Modelling Simul. Mater. Sci. Eng.* **6** (1998) 349.

[8] M. Seefeldt, V. Klemm and P. Klimanek, in: *Investigations and Applications of Severe Plastic*

Deformation, Proceedings of the NATO Advanced Research Workshop, edited by T.C. Lowe and R.Z. Valiev (Kluwer, Dordrecht, 1999), in print.
[9] R. de Wit // *J. Res. Natl. Bur. Stand*. (US) A **77** (1973) 49, 359 and 607.
[10] A.E. Romanov and V.I. Vladimirov, Disclinations in Crystalline Solids, in: *Disclinations in Solids*, vol. **9**, edited by F.R.N. Nabarro (North Holland, Amsterdam, 1992) p. 191.
[11] V.I. Vladimirov and A.E. Romanov // *Fiz. Tverd. Tela* **20** (1978) 3114.
[12] V. Klemm, P. Klimanek and M. Seefeldt // *Phys. Stat. Sol*. (a) **175** (1999) 569.
[13] V.V. Rybin, N.Yu. Zolotorevskiy and I.M. Zhukovskiy // *Fiz. Met. Metalloved*. **69** (1990) 5.
[14] V.V. Rybin, A.A. Zisman and N.Yu. Zolotorevskiy // *Acta Metall. Mater.* **41** (1993) 2211.
[15] V. Klemm, P. Klimanek and M. Seefeldt, to be published.
[16] V.I. Vettegren', S.Sh. Rakhimov and V.N. Svetlov // *Fiz. Tverd. Tela* **37** (1995) 913.
[17] V.I. Vettegren', S.Sh. Rakhimov and E.A. Bakulin // *Fiz. Tverd. Tela* **37** (1995) 3630.
[18] V.I. Vettegren', S.Sh. Rakhimov and V.N. Svetlov // *Fiz. Tverd. Tela* **37** (1995) 3635.
[19] V.I. Vettegren', S.Sh. Rakhimov and V.N. Svetlov // *Fiz. Tverd. Tela* **38** (1996) 590.
[20] V.I. Vettegren', S.Sh. Rakhimov and V.N. Svetlov // *Fiz. Tverd. Tela* **38** (1996) 1142.
[21] V.I. Vettegren', V.L. Gilyarov, S.Sh. Rakhimov and V.N. Svetlov // *Fiz. Tverd. Tela* **40** (1998) 668.
[22] T.T. Tsong // *Phys. Rev. B* **44** (1991) 13703.
[23] W.W. Mullins // *J. Appl. Phys.* **28** (1957) 333.
[24] P. Paufler and G.E.R. Schulze, *Physikalische Grundlagen mechanischer Festkorpereigenschaften I* (Akademie-Verlag, Berlin, 1978).
[25] A.E. Romanov // *Poverkhnost'* **6** (1982) 121.
[26] D.A. Hughes and N. Hansen // *Mater. Sci. Technol*. **7** (1991) 544.